

THE EFFECTS OF PRELOAD AND NONLINEARITY ON THE VIBRATION OF RAILWAY TRACKS UNDER HARMONIC LOAD

Samuel G. Koroma*¹, Mohammed F.M. Hussein², John S. Owen²

¹University of Nottingham, University Park, Nottingham, NG7 2RD, UK
evxsgk1@nottingham.ac.uk

²University of Nottingham, University Park, Nottingham, NG7 2RD, UK
{mohammed.hussein,john.owen}@nottingham.ac.uk

Keywords: Railpad stiffness and damping, Preload and frequency dependence, Poynting-Thomson model.

Abstract. *Railway tracks are commonly constructed with resilient elements (railpads, ballasts etc.) that attenuate the level of impact of railway vehicles on the tracks. Being vibration reduction methods at the source, they serve as the primary means of reducing the level of vibration generated through railway operations. The properties of these resilient elements (stiffness and damping) have significant effects on the track vibration and the forces transmitted to the track supporting infrastructure and the underlying soil. In modelling the dynamic behaviour of railway tracks, the most common assumption adopted by many authors is that the stiffness and damping properties of the resilient components are linear and homogeneous throughout the length of track; i.e. independent of the state and loading history of the track. However, some studies by [1] and [2] show that resilient elements exhibit pronounced nonlinear behaviour and their properties are dependent on preloads as well as frequency.*

In this paper, a nonlinear finite element model has been presented for a rail that is discretely supported on railpads with nonlinear stiffness under combined static and dynamic load to study the effects of preload and nonlinearity on railway track dynamics. The rail is modelled using Euler-Bernoulli beam elements whereas the railpads are modelled using a three parameter model that comprises of a frequency independent spring in parallel with both a frequency dependent spring and dashpot. The latter two parameters are in series with other, with the springs representing the railpad stiffness and dashpot the damping properties respectively. The problem is solved using a composite implicit time integration scheme.

Results are plotted for the maximum rail displacement versus frequency for various preload levels. It can be summarised that the effect of preload on the dynamic response of the track is a reduction in the response amplitude and an increase in the track resonance frequency due to the increased stiffness of the track.

1 INTRODUCTION

Railway tracks are commonly constructed with railpads that attenuate the level of vibration and impact transmitted to them from railway vehicles. The stiffness and damping properties of railpads greatly affect the level of track vibration and forces transmitted to the track substructure and subsequently to the underlying soil. When modelling track dynamic behaviour, it is most common to assume that these properties are linear and homogeneous. However, many studies, including [1, 2, 3, 4], etc., have shown that railpads exhibit pronounced nonlinear behaviour and their properties are dependent on preload and frequency. Characterising these dependencies is, to a large extent, subjective to a particular data set and is by no means a generic process. Therefore, this process should be carried out with the scope set to particular applications, for e.g. in railway track dynamics, the scope may be to predict the vibration levels in a track for which experimental data is available for the railpads.

The preload dependent behavior of a railway track with nonlinear railpads and ballast was studied by [5]. The preload dependent stiffnesses of the railpads were calculated using an equivalent continuous elastic foundation model. These were then used in a discretely supported track model in the frequency domain to obtain the track receptances and decay rates. However, the two parameter railpad model that was used failed to account for the loading rate (i.e. frequency of excitation).

In this paper, the static and dynamic properties of the railpad are modelled using a three parameter Poynting-Thomson (P-T) model. In section 2, empirical expressions for the static and dynamic stiffnesses for a railpad are derived based on experimental data presented by [2]. A time domain based nonlinear Finite Element model is then developed in section 3, which incorporates the nonlinear railpads. The model consists of a rail that is discretely supported on railpads with preload and frequency dependent stiffness and damping under combined static and dynamic load. The model is solved in the time domain using a time integration scheme. Results are presented for the track dynamic displacement and reaction force for various preload levels and over a frequency range of up to 500 Hz.

2 RAILPAD STIFFNESS AND DAMPING PROPERTIES

In this section, the static and dynamic load-displacement relationship of a railpad is presented. Based on experimental data presented in [2], empirical approximation is done for both the static and dynamic stiffnesses of a railpad using a three parameter P-T visco-elastic model, see [3]. This model consists of a frequency independent spring that is in parallel with a series combination of spring and dashpot. The latter two parameters ensure that the frequency dependence of the load is accounted for, as will be shown later from the differential equation of motion. In this model, the spring represents the stiffness and the dashpot the damping of the railpad. Section 2.1 deals with the static stiffness whilst section 2.2 deals with the dynamic stiffness.

2.1 Static stiffness of railpads

In this section, the characterisation of a railpad's load-displacement relationship, and hence its static stiffness is described. For static loading conditions, the railpad is assumed to behave purely as an elastic material with nonlinear load-displacement relationship. The static force, p_{st} , on the railpad is a nonlinear function of the displacement, u_{st} , and can be characterised by a polynomial of degree α such that

$$p_{st}(u_{st}) = k_1 u_{st} + k_2 u_{st}^2 + \dots + k_j u_{st}^j + \dots + k_\alpha u_{st}^\alpha, \quad (1)$$

where k_1, \dots, k_α are the coefficients of the polynomial and are obtained through the nonlinear curve fitting of experimental data, and j is a positive integer. In order to ensure that the fit between p_{st} and u_{st} is well conditioned, the approximation is done with p_{st} being in kN and u_{st} in mm.

From Eq. (1), two types of stiffness can be obtained; the secant stiffness, $k_s = \Delta p_{st} / \Delta u_{st}$, and the tangent stiffness, $k_t = dp_{st} / du_{st}$.

A seventh degree polynomial was found to sufficiently describe the $p - u$ relationship given in [2]. The values of the coefficients are $k_1 = 20.00$, MN/m, $k_3 = 3.94$ MN/m³, $k_5 = -1.78$ MN/m⁵ and $k_7 = 3.28$ MN/m⁷. The coefficients of the polynomial that are not included here are zeros. Note that when fully unloaded, the railpad possesses an unloaded stiffness of k_1 MN/m.

In the construction of railway tracks, each railpad is preloaded by clips that hold it in place and by the weight of the rail that is supported within one fastener bay (i.e. 0.6 m length of rail). Wu and Thompson [5] calculated the total force to be about 20.36 kN, for 60E1 rail. To account for this initial preload, the reaction force in the railpad due to external track loads are added to this preload. However, it is assumed that the railpad is in static equilibrium at this preload, and all displacements are taken with reference to this point.

2.2 Dynamic stiffness and damping of railpads

In addition to the dependence of a railpad's stiffness on preload as outlined in the previous section, the stiffness is also dependent on frequency. Some data of the dynamic stiffness of railpads obtained from laboratory measurements have been presented by [1, 2, 4] for studded rubber railpads that are commonly used in European railways. In [2], the dynamic stiffness values are given for five preload levels: 20, 30, 40, 60, and 80 kN, over a frequency range of 40-1000 Hz. Using this data, approximations of the dynamic stiffness as a function of preload and loading rate are derived using nonlinear curve fitting.

Fig. 1 shows a Poynting-Thompson railpad model subjected to a force, p , with a corresponding displacement, u .

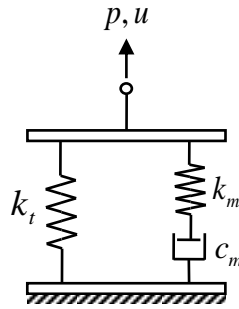


Figure 1: Poynting-Thomson model for a railpad with nonlinear elastic spring of stiffness k_t in parallel with a series combination of spring of stiffness k_m and dashpot of damping factor c_m

The differential equation of motion is derived by considering compatibility and equilibrium of the elements of the model. The parallel arrangement of the two branches of P-T model ensures a common displacement, u , between them but the total force p is the sum of the reaction forces in the two branches (denoted as p_t and p_m for the left and right branch respectively). Also, the series arrangement in the right branch means that the force, p_m , is mutual but the total displacement is a sum of that in the spring and dashpot. Using these conditions, one obtains the

following equation

$$\dot{p} + \frac{k_2}{c_m} p = \left(k_m + \frac{dp_t}{du} \right) \dot{u} + \frac{k_m}{c_m} p_t, \quad (2)$$

Equation (2) governs the dynamic behaviour of the P-T railpad model and can be seen to contain terms of rate of loading. These terms capture the frequency dependent behaviour of the railpad.

Consider the force, p , to be composed of a static preload, p_{st} , and a dynamic load p_{dyn} . The resulting tangent stiffness due to the preload is $k_t = \frac{dp_t}{du}$, due to the nonlinear $p - u$ curve relationship. Assuming that the dynamic behaviour is linear (i.e. independent of the dynamic load amplitude), the dynamic part of p_t is then $k_t u_{dyn}$, where u_{dyn} is the dynamic displacement. Now, if p_{dyn} varies harmonically, then the resulting dynamic stiffness of the railpad is derived to be

$$k_{dyn} = k_t \left[1 + \frac{k_m}{k_t} \frac{i\omega_0\tau}{1 + i\omega_0\tau} \right] \quad (3)$$

The parameters k_m and c_m are obtained from nonlinear curve fitting. The values obtained for k_m and c_m from the optimisation show some preload dependence, in accordance with the following equations

$$k_m = k_{m0}(1 + \beta^r), \quad (4a)$$

$$c_m = c_{m0}(1 + \beta^s) \quad (4b)$$

where k_{m0} and c_{m0} are the respective values of k_m and c_m at a reference preload value p_c , $k_{m0} = 60.33 \times 10^6$ N/m and $c_{m0} = 22.50 \times 10^4$ N.s/m. r and s are the exponential preload influence and are almost identical ($r = 1.9954$ and $s = 2.07$), but for simplicity a value of 2 is used for both of them. The reference preload is taken as 20.36 kN, as calculated by [5].

Approximations of k_{dyn} in (3) for the P-T model, together with the optimised parameters, are plotted in Fig. 2 against frequency for five preload levels. It can be seen in Fig. 2 that there

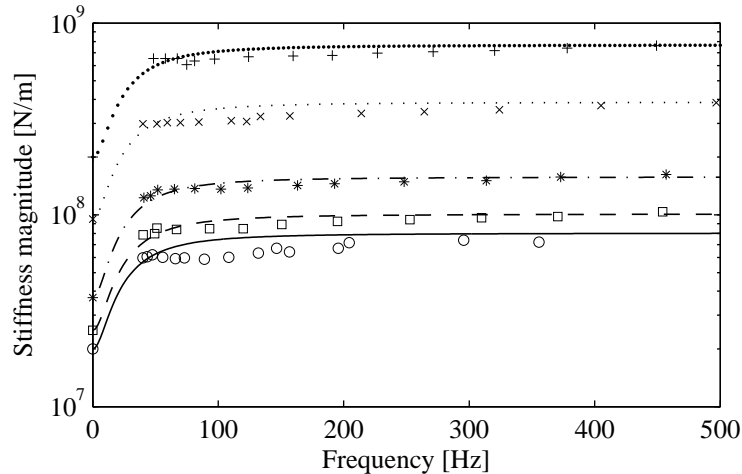


Figure 2: Approximations of railpad dynamic stiffness according to t P-T model, plotted against frequency for various preload levels (lines) compared with data points from [2] (markers). —, o: 20; - - -, □: 30; - · - ·, *: 40; ·····, ×: 60 and ·····, +: 80 kN

is a good agreement between Eq. (3) and the experimental data. Although experimental data is not available between 0 – 40 Hz, it is assumed for the P-T model that the dynamic stiffness

increases gradually from a value of k_t at 0 Hz to the value at 40 Hz, disregarding any resonance that may be present within this range.

In the next section, the P-T railpad model is incorporated into a Finite Elements based track model.

3 NONLINEAR FINITE ELEMENT TRACK MODEL

3.1 Model description

Fig. 3 is a time domain Finite Elements (FE) based model of a railway track in which the rail is modelled as an Euler-Bernoulli beam with bending stiffness, EI , and mass per unit length, m . The rail is discretely supported on railpads at regular intervals, d , (typically 0.6 m) and is simply supported at the ends. The railpads are modelled using the three parameter P-T model discussed in the previous section. For the purpose of studying only the effects of railpad properties on the dynamic behaviour of the track, it assumed that all track layers below the railpads are much stiffer than the railpads and can therefore be assumed to be rigid.

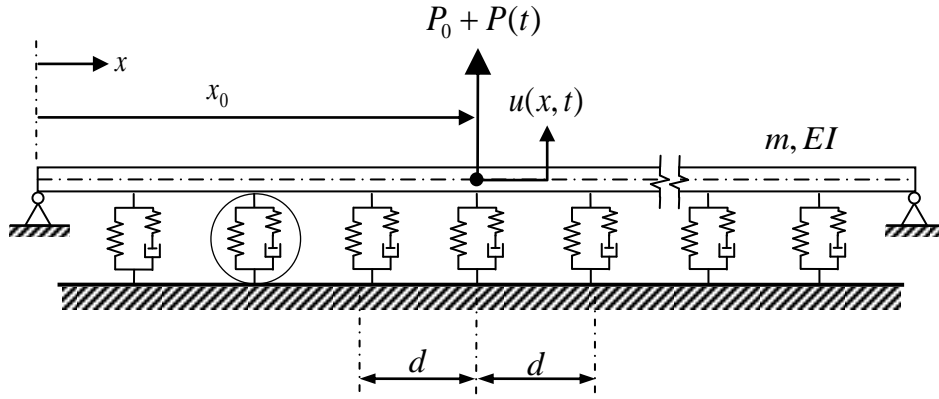


Figure 3: Rail discretely supported on a three parameter P-T elastic foundation and subjected to combined static and dynamic load

The track is subjected to a non-moving load, $P_{tot}(t)$ placed at a fixed point, a distance of x_0 from the left end of the track. The load consists of a static component, P_0 , and a dynamic component, $P(t)$. In order to investigate the dynamic behaviour of the track, $P(t)$ is defined as a harmonic function with amplitude, P_1 and angular frequency $\omega_0 = 2\pi f_0$, f_0 being the excitation frequency. Hence, the load on the track can be described by

$$P_{tot}(t) = [P_0 + P_1 e^{i\omega_0 t}] \delta(x - x_0), \quad (5)$$

where $x_0 = NL/2$ corresponds to the middle node of the beam, directly on a railpad.

3.2 Discretisation of the beam and system matrices

The rail is discretised into N finite elements, each having two nodes and four degrees-of-freedom (dofs), i.e. a vertical translation and rotation at each node. The length of each of these elements, L , is chosen such that $d/L = q$, where q is a positive integer. Let the number of railpad bays that is included in the track model be n , so that the number of railpads, $N_R = n + 1$. The total number of elements in the track structure is therefore $N = n \times q$, the number of nodes is $N + 1$ and the total number of dofs $N_D = 2(N + 1)$.

The local stiffness and consistent mass matrices for the i th beam element are denoted by $\mathbf{K}_{B,i}$ and \mathbf{M}_i respectively. The assembly of the system matrices is done in the next section.

3.3 Assembly of global matrices for the beam

The global stiffness and mass matrices of the beam structure are assembled using compatibility conditions at the nodes, i.e. displacement, slope and bending moments are continuous. In this way, the local matrix components corresponding to the mutual nodes between two successive elements are overlapped. The assembly of the global matrices can be summarised in the following equations:

$$\mathbf{K}_B = \sum_{i=1}^N \tilde{\mathbf{K}}_{2i-1:2i+2, 2i-1:2i+2} + \mathbf{K}_{B,i} \quad (6)$$

$$\mathbf{M} = \sum_{i=1}^N \tilde{\mathbf{M}}_{2i-1:2i+2, 2i-1:2i+2} + \mathbf{M}_i \quad (7)$$

where $\tilde{\mathbf{K}}$ and $\tilde{\mathbf{M}}$ are $N_D \times N_D$ null matrices for the stiffness and mass of the beam respectively.

In addition to the global mass and stiffness matrices for the rail/ beam, global stiffness and damping matrices of the railpads should also be formed and coupled to the beam in order to obtain the global matrices of the track structure. The coupling of the beam to the railpads and formulation of the equation of motion for the entire track structure are carried out in the next section.

3.4 Equation of motion of the track

The coupling of the rail (beam) to the railpads requires the formulation of the differential equations for the individual systems and using compatibility to obtain the overall equation of motion of the track. The differential equations of the beam and the railpad become

$$\mathbf{M}\ddot{\mathbf{u}} + \mathbf{K}_B\mathbf{u} + \mathbf{F} = \mathbf{P}, \quad (8a)$$

$$[\mathbf{K}_M + \mathbf{K}_T]\dot{\mathbf{u}}_P + \frac{1}{\tau}\mathbf{K}_T\mathbf{u}_P = \frac{1}{\tau}\mathbf{F}_P + \dot{\mathbf{F}}_P, \quad (8b)$$

where \mathbf{u}_P and \mathbf{F}_P are $N_R \times 1$ vectors that contain the vertical displacements and reaction forces of the nodes at which the railpads are located, therefore they are subsets of the global beam displacement and reaction force vectors, \mathbf{u} and \mathbf{F} . \mathbf{K}_M and \mathbf{K}_T are $N_R \times N_R$ diagonal matrices containing the k_{m_j} and k_{t_j} values of the railpads respectively, for $j = 1, 2, \dots, N_R$. The relaxation time $\tau = c_{m0}/k_{m0}$, since the preload influence for both the stiffness and damping of the right branch is the same.

The presence of the load rate $\dot{\mathbf{F}}_P$ in Eq. (8b) prevents a simple substitution of the railpad matrices into the beam matrices. Therefore, the coupling is sought by making \mathbf{F}_P part of the global unknown vector of the track system. By assembling Eqs. (8a) and (8b) into matrix form, the coupled system equation can be formed as follows

$$\begin{bmatrix} \mathbf{M} & \mathbf{0} \\ \mathbf{0} & \mathbf{0} \end{bmatrix} \begin{Bmatrix} \ddot{\mathbf{u}} \\ \dot{\mathbf{F}}_P \end{Bmatrix} + \begin{bmatrix} \mathbf{0} & \mathbf{0} \\ \mathbf{A} & -\mathbf{I} \end{bmatrix} \begin{Bmatrix} \dot{\mathbf{u}} \\ \dot{\mathbf{F}}_P \end{Bmatrix} + \begin{bmatrix} \mathbf{K}_B & \mathbf{J} \\ \frac{1}{\tau}\mathbf{B} & -\frac{1}{\tau}\mathbf{I} \end{bmatrix} \begin{Bmatrix} \mathbf{u} \\ \mathbf{F}_P \end{Bmatrix} = \begin{Bmatrix} \mathbf{P} \\ \mathbf{0} \end{Bmatrix} \quad (9)$$

The coupled system in Eq. (9) has the same number of dofs N_D but the number of unknowns is $N_D + N_R$. The sub matrices are defined as follows: \mathbf{A} and \mathbf{B} are $N_R \times N_D$ matrix with

non-zero elements $\mathbf{A}_{j,2q(j-1)+1} = \mathbf{K}_{M_{j,j}} + \mathbf{K}_{T_{j,j}}$, and $\mathbf{B}_{j,2q(j-1)+1} = \mathbf{K}_{T_{j,j}}$. \mathbf{J} is a $N_D \times N_R$ matrix that contains unit values only at the dofs corresponding to the positions of the railpads, i.e. $\mathbf{J}_{2q(j-1)+1,j} = 1$, for $j = 1, 2, \dots, N_R$, and \mathbf{I} is an identity matrix of size $N_R \times N_R$.

3.5 Solution of the equation of motion of the track

The procedure for solving the differential equations of motion for the FE model is to first determine the preloaded stiffnesses of the railpads, calculated based on the static load-deflection relationship and according to the magnitude of the static load. These are then used as input to study the dynamic behaviour of the track. The first part is considered in section 3.5.1, whilst solution for the dynamic response is discussed in section 3.5.2.

3.5.1 Calculation of preloaded stiffnesses

To obtain the preloaded stiffnesses of the railpads under the effect of the static load, the following nonlinear static equation needs to be solved

$$\mathbf{F}(\mathbf{u}_0) = \mathbf{P}_0, \quad (10)$$

where $\mathbf{F}(\mathbf{u}_0)$ is the nonlinear reaction force vector; $\mathbf{F}(\mathbf{u}_0) = \mathbf{K}(\mathbf{u}_0)\mathbf{u}_0$, with $\mathbf{K}(\mathbf{u}_0)$ being the nonlinear static stiffness as a function of the static displacements \mathbf{u}_0 . \mathbf{P}_0 is the external nodal force vector consisting of P_0 as the only non-zero element, at the corresponding dof where the external load is applied.

A simple Newton-Raphson iteration procedure is adopted to obtain the static displacements of the pads, and hence the preloaded stiffnesses. This procedure is summarised as

$$\begin{aligned} \mathbf{K}^{(i-1)}\Delta\mathbf{u}_0^{(i)} &= \mathbf{P}_0 - \mathbf{F}^{(i-1)} \\ \mathbf{u}_0^{(i)} &= \mathbf{u}_0^{(i-1)} + \Delta\mathbf{u}_0^{(i)} \end{aligned} \quad (11)$$

where $\mathbf{K}^{(i-1)}$ and $\mathbf{F}^{(i-1)}$ are respectively the consistent tangent stiffness matrix and reaction force vector computed at the configuration corresponding to the static displacement $\mathbf{u}_0^{(i-1)}$, for i being the number of iterations. Convergence of Eq. (11) is achieved by satisfying a predefined convergence criterion that guarantees the degree of accuracy required for the solution.

Table 1 contains the static preloads for the case when a static load is positioned directly over a railpad. Due to symmetry, only the railpads on one side of the load have been presented.

It can be seen from Table 1 that when there is no load on the track, all pad preloads are equal to the unloaded value 20.36 kN. They then increase for higher levels of preload and beyond a distance of about 3–4 m from the load, the pads are almost insensitive to load and remain fairly unloaded.

3.5.2 Solution for the dynamic response

Once the preloaded stiffnesses have been obtained, the differential equation is solved only for the dynamic loading, with the complete solution being a sum of the static and dynamic parts. The solution is obtained using the composite implicit time integration scheme presented by [6].

4 RESULTS AND DISCUSSIONS

In this section, results are presented for the nonlinear FE model to study the effect of preload and frequency on track dynamics. Five levels of static load are considered; 0, 25, 50, 75 and 100

Table 1: Preloads (in kN) on the railpads in the vicinity of the static load

Pad position from load (m)	Static Load (kN)					
	0.00	25.00	50.00	75.00	100.00	125.00
0.00	20.36	28.47	37.26	48.24	62.57	79.40
0.60	20.36	26.26	32.09	37.41	41.75	45.29
1.20	20.36	23.08	25.56	27.50	28.73	29.49
1.80	20.36	21.04	21.62	22.03	22.24	22.34
2.40	20.36	20.18	20.00	19.83	19.69	19.58
3.00	20.36	20.02	19.70	19.45	19.28	19.16
3.60	20.36	20.12	19.91	19.74	19.63	19.56
∞	initial preload of 20.36					

kN. Superimposed on each of these is a unit amplitude dynamic load. The preloaded stiffness distribution is calculated using Eq. (11) and then used as input to study the dynamic response.

Fig. (4) shows the dynamic displacement amplitude and phase as a function of excitation frequency for a point that is directly under the load. The displacement initially reduces from its

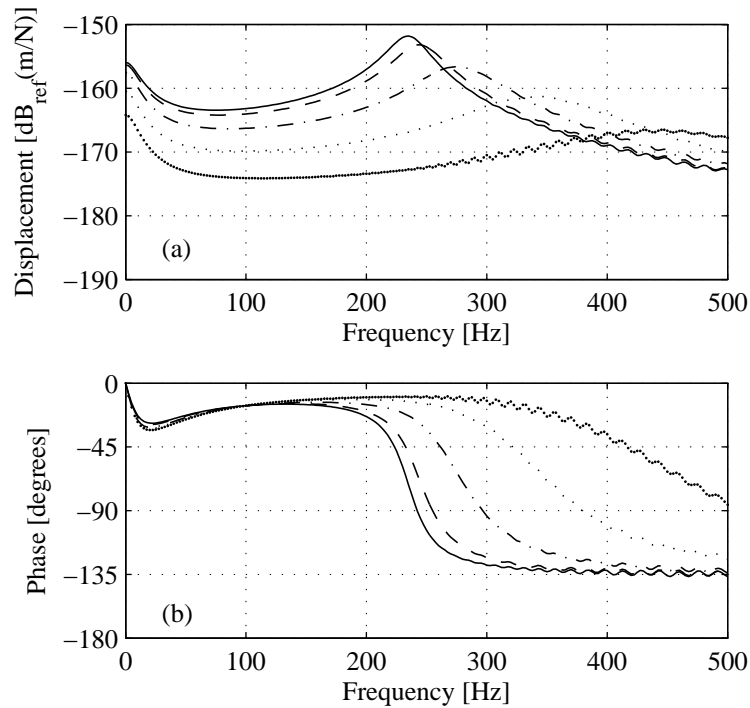


Figure 4: (a) Steady-state displacement amplitude and (b) phase angle for a point directly under the load plotted against frequency of the oscillating load for five preload levels. —: 0 kN, - - -: 25 kN, - · - ·: 50 kN, · · · ·: 75 kN and · · · ·: 100 kN

value at 0 Hz by more than 7.5 dB for some preload levels up to a frequency of 80-100 Hz. At this stage the dynamic stiffness of the railpad increases sharply, at a higher rate than the dynamic reaction force on the railpad. This difference in rates of increase in the dynamic resistance and force causes a reduction in the response. However, as the frequency increases, the inertial force

from the rail becomes increasingly dominant, leading to an increase in the response up until the resonance frequency. The track displacement then gradually decays beyond this point.

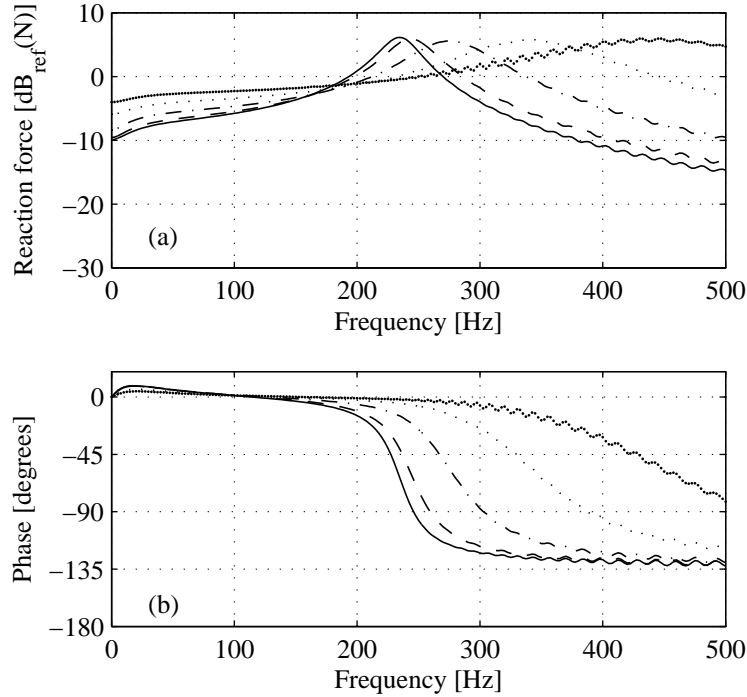


Figure 5: (a) Steady-state reaction force amplitude and (b) phase angle at a point directly under the load plotted against frequency of the oscillating load for five preload levels. Key as for Fig. 4

As the magnitude of the static load increases, the response amplitudes decrease due to the higher tangent stiffness induced by the load on the railpads in its vicinity. It can be seen that, for some frequencies, there is a difference of more nearly 20 dB between the linear case of 0 kN preload and the strongly nonlinear case of 100 kN. The increased stiffness also leads to increased resonance frequencies.

In Fig. (5), as the preload increases, the railpads become stiffer and the proportion of the static load that goes into the railpad directly underneath it increases from about 32% at 25 kN to 42% at 100 kN (see Table 1 for details). Although the maximum reaction forces at resonance remain fairly constant, the dynamic amplification reduces as preload increases. The dynamic amplification is the ratio of the peak reaction force at any given frequency to that at 0 Hz.

5 CONCLUSIONS

In this paper, a nonlinear railpad model has been developed and incorporated into an FE based model of a railway track to study the effects that preload and frequency have on its dynamic behaviour. The key conclusions are summarised as follows:

- The main effect of the static preload is to induce a loaded stiffness distribution of the railpads in its vicinity, due to the nonlinear load-displacement relationship. Depending on the magnitude of the static load, this distribution may exhibit much higher stiffness of the railpads close to the load, whereas those about 3 – 4 m from the load remain unloaded with linear parameters.

- As the preload increases, the railpads become much stiffer than their initial linear value hence resulting in lower response amplitudes. For static loads of up to 100 kN, the use of a constant linear parameter railpad model results in an overestimation of the track dynamic response amplitudes of up to 20 dB for some frequencies, compared to the nonlinear model.

REFERENCES

- [1] A. Fenander. Frequency dependent stiffness and damping of railpads. *Proceedings of the Institution of Mechanical Engineers*, 211(Part F):51–62, 1997.
- [2] D.J. Thompson, W.J. van Vliet, and J.W. Verheij. Development of an indirect method for measuring the high frequency dynamic stiffness of resilient elements. *Journal of Sound and Vibration*, 213(1):169–188, 1998.
- [3] A.P. De Man. *Dynatrack: a survey of dynamic railway track properties and their quality*. PhD thesis, TU Delft, Delft, 2002.
- [4] J. Maes, H. Sol, and P. Guillaume. Measurements of the dynamic railpad properties. *Journal of Sound and Vibration*, 293:557–565, 2006.
- [5] T. X. Wu and D.J. Thompson. The effects of local preload on the foundation stiffness and vertical vibration of railway track. *Journal of Sound and Vibration*, 219(5):881–904, 1999.
- [6] K-J Bathe and M.M. Irfan Baig. On a composite implicit time integration procedure for nonlinear dynamics. *Computers and Structures*, 83:2513–2524, 2005.